Assessing porewater and sediment quality in the Sidi Salem Dam: insights from an artificial aquatic geosystem in Tunisia

Mohamed Amine Helali, Imen Ouameni, Haifa Ben Mna, Valérie Mesnage, Radhia Souissi, Ahmed Kouka, Walid Oueslati

applied sciences

MDPI

Article

A Relevant Characterization and Compatibility for Reuse the Sediments from Reservoirs in Southern Italy

Audrey Maria Noemi Martellotta [1,2,*], Daniel Levacher [3,*], Francesco Gentile [1], Gennaro Ranieri [2], Teresa Trabace [4] and Alberto Ferruccio Piccinni [2]

[1] Department of Soil, Plant and Food Sciences, University of Bari Aldo Moro, Via Amendola 165/A, 70126 Bari, Italy; francesco.gentile@uniba.it
[2] Department of Civil, Environmental, Land, Building Engineering and Chemistry, Polytechnic University of Bari, Via E. Orabona 4, 70125 Bari, Italy; gennaro.ranieri@poliba.it (G.R.); albertoferruccio.piccinni@poliba.it (A.F.P.)
[3] Continental and Coastal Morphodynamics -M2C, UMR 6143 CNRS-, University of Caen Normandy, 24 rue des Tilleuls, 14000 Caen, France
[4] ARPA Basilicata, S.S. 106 Km 2 Zona Pantanello MT, 75012 Metaponto, Italy; teresa.trabace@arpab.it
* Correspondence: audreymarianoemi.martellotta@poliba.it (A.M.N.M.); daniel.levacher@unicaen.fr (D.L.)

Abstract: The damming of watercourses results in sediment accumulation and, therefore, in the reduction of useful storage capacity. The storage capacity can be recovered through dredging, but this process generates large volumes of sediments that require proper management. To avoid landfilling and promote recovery operations, sediment characterization is the preliminary step to any assessment and decision. This paper presents the results of tests on sediments sampled at two reservoirs in southern Italy, the Camastra and the San Giuliano, in Basilicata. These investigations include testing of organic matter, heavy metals grain size distribution, and the assessment of the pollution degree. A lack of correlation between the sampling point and the heavy metal content was observed in sediments, except Be, Cr and Ni for the San Giuliano reservoir. This may be attributed to the presence of agricultural activities and fertilizer use in its watershed. Similarly, there is no dependence between the organic carbon and the grain size distribution, the former being scarcely found in both reservoirs (on average 0.91% for the Camastra sediments and 0.38% for the San Giuliano sediments), the latter being predominantly characterized by sandy matrices downstream of the reservoirs (on average 64.3% ± 32.9%) and by silty-clayey matrices in the upstream areas (on average 65% ± 14.3%). Finally, the determination of the single pollution index P_i and the Nemerow integrated pollution index P_N highlights that sediments are not contaminated with heavy metals. Most of them show values of the indices above between 0 and 1 ("unpolluted") and, in a few cases, values between 1 and 2 ("poorly polluted"). The findings suggest that these sediments can be reused for environmental and material recovery, using them as secondary raw materials for sub-bases and embankments, for filling in disused quarries, for reprofiling and reconstructing the morphology of coastlines or riverbeds, for beach nourishment and in the agronomic and construction industry fields.

Keywords: sediment reuse; dredged sediment; statistical analysis; sediments pollution; heavy metals

Citation: Martellotta, A.M.N.; Levacher, D.; Gentile, F.; Ranieri, G.; Trabace, T.; Piccinni, A.F. A Relevant Characterization and Compatibility for Reuse the Sediments from Reservoirs in Southern Italy. *Appl. Sci.* **2024**, *14*, 727. https://doi.org/10.3390/app14020727

Received: 19 December 2023
Revised: 6 January 2024
Accepted: 11 January 2024
Published: 15 January 2024

1. Introduction

Artificial reservoirs, which man has built since time immemorial to store water for drinking, irrigation, industrial uses, etc., are the main reservoirs of water resources, and the societies that develop around them depend heavily on their sustainability [1–5]. However, dams constitute a substantial interference with the water outflow and affect the phenomenon of solid transport, as they interrupt the regular flow of materials produced by water erosion on the banks and the bottom. In this way, sediments can no longer reach the estuary but are retained upstream of the dam, accumulating on the bottom,

and reducing, over time, the useful reservoir capacity due to an upstream area with reduced velocities [6–10]. This capacity may be sustainable or exhaustible, depending on whether sediment management plans are established, and recovery measures are implemented [11,12]. In this regard, the strategies currently employed to accept the phenomenon of sediment accumulation passively are not sustainable in the long term [13,14]. The aim, on the contrary, should be to achieve a balance whereby, in addition to accepting that part of the usable capacity is taken away, thresholds should be set, at which the breakthrough processes are initiated [15,16]. The volume recovery operations, functional to maximize the water holding capacity of the reservoir necessitate the removal of sediments deposited at the bottom of the reservoir. However, the challenge of disposal remains, since dredged sediments are classified as waste. Italian legislation, however, in agreement with European directives, allows alternative options if it is guaranteed that the sediment, in being reused, does not present a risk to each of the main ecosystem components [17].

Characterization of the dredged sediment becomes essential, i.e., defining a complete set of analyses that provides the necessary information to determine the reuse of sediments. It is possible to propose and verify the compatibility of sediments for environmental recovery, to use the dredged material for nourishment of coastlines and sandy shores, for filling disused quarries or for making road embankments and subgrades, and for material recovery, especially in those production sectors with the most significant environmental impact, such as agriculture and the building materials industry [18,19]. Therefore, it is essential to define its physical, chemical, and mineralogical properties, to assess its compatibility for reuse in the construction materials field [20–24]. In addition, investigations to quantify the organic matter, nutrient, sodium, and salinity content are equally important for sediment reuse in agronomic applications [25,26]. In any case, whatever the hypothesis of reuse, a complete characterization of dredged sediments cannot ignore analyses of water content and the content of contaminants whose presence in high concentrations may constitute an obstacle to their reuse [27–29].

However, dredging and sediment characterization have significant economic and environmental costs, so the possibility of reuse may not represent an economically viable alternative [30]. Therefore, it is the task of scientific research to identify sustainable solutions, both environmentally and economically, to make it worthwhile to dredge the sediment, characterize it thoroughly, and give it new life, thereby preserving the non-renewable natural resources and reducing the carbon footprint of some of today's most impactful production fields [26].

This research focuses on characterizing sediments sampled at two reservoirs in the Basilicata region of southern Italy, known as the San Giuliano reservoir and the Camastra reservoir. Analyses of the materials show that heavy metals are often below the main regulatory reference limits [31]. In addition, the organic matter content is, on average, below 2%, a value considered the organic matter content below which the sediment cannot ensure nutritional and structural functions and guarantee adequate fertility in a possible hypothesis of reuse in an agronomic context. In addition, the research aimed to examine the possible influence of grain size distribution and land use on the heavy metal and total organic carbon contents, a topic already discussed in other papers [32–39], to identify a potential relationship that could allow for the limitation of characterization activities which are quite expensive. This was generally not the case, but only for some parameters; the statistical analyses show that the area of origin and its characteristics directly influence the heavy metal and the total organic carbon contents. Finally, starting from the values of the primary contaminants, it was possible to derive the single-factor pollution index and Nemerow's integrated pollution index [40], which made it possible to specify the degree of contamination of the sampled sediments [41,42].

2. Materials and Methods

2.1. Study Area

The Basento river is closed off from its right-hand tributary, the Camastra river, by the dam of the same name downstream of its confluence with the Inferno river. The area of the watershed, which tributes its waters to the Basento river, the longest in Basilicata (149 km), is 1535 km^2 and has predominantly mountainous to hilly morphological features up to the flat areas found near the Basento riverbed and the Ionian coast.

The Basento river receives the waters of the Camastra river (25 km long) on the hydrographical right, on which the Camastra reservoir is located, in the valley between Trivigno, Anzi, Laurenzana, and Albano di Lucania, in the Ponte Fontanelle area. The Camastra reservoir watershed covers 341 km^2, occupying approximately 3.4% of the region's total surface area. The terrain of the basin is high in the west and south, low in the east and north, sloping from southwest to northeast, with a significantly articulated hydrographical system with brooks and valleys, often steep-sided. The average annual runoff is approximately 20.0 Mm^3. The catchment area subtended by the dam is affected by dolomitic limestones, crystalline dolomites, arenaceous limestones and siliceous schists (Triassic formations), white and grey limestones (Cretaceous formations), nummulitic breccias argillaceous schists, variegated scaly clays, marly and nummulitic limestones, hard and soft sandstones, conglomerates of crystalline rocks (Middle Lower Tertiary formations), from yellow marine sands (post-Pliocene) and present-day alluvium.

The Camastra reservoir (located according to the position shown in Table 1) belongs to the temperate and cold climate with a rainfall regime that is exposed to disturbances from the west and northwest and has an average annual rainfall of 750 mm, with the months with the highest rainfall being November and December, and the months with the lowest rainfall being July and August. The rainfall pattern is subject to substantial variations, with a considerable part of the rainfall concentrated in a few days, with high intensity.

Table 1. Camastra reservoir coordinates.

N-W	15°39′30.12″ E	40°38′41.55″ N
N-E	16°06′48.23″ E	40°38′41.55″ N
S-E	16°06′48.23″ E	40°17′19.92″ N
S-W	15°39′30.12″ E	40°17′19.92″ N

The artificial dam, made of earth with an impermeable central core, has a depth of 54 m and is located at an elevation of 495 m above sea level. The water drawn from it is used to meet the drinking water needs of the city of Potenza and its hinterland (15 Mm^3). It also meets the water requirements of the Val Basento industrial area (2 Mm^3) and the irrigation sector along the Basento river floodplains (3 Mm^3).

Also, in the same region, there is another site under investigation: The San Giuliano artificial reservoir, originating from the dam on the Bradano river at San Giuliano, in the municipalities of Grottole, Matera, and Miglionico, the first of Basilicata's rivers in terms of the dimensions of its hydrographic basin. The watershed of the Bradano river, included the basin of the Ofanto river to the northwest, the basins of Puglia's regional watercourses with outlets in the Adriatic Sea and the Ionian Sea to the northeast and east, and the basin of the Basento river to the south, has a surface area of 3037 km^2. The watercourse has a length of 116 km and primarily extends into Lucanian territory, except for a limited part near the outlet, which falls within Apulian territory. Near the San Giuliano lake, it alternates the appearance of a fiumara with a serpentine course.

The dam, comprising a catchment basin of 1262 km^2, is made of concrete of the gravity type, with a depth of 38.3 m, and is placed at a riverbed elevation of 67 m above sea level. The San Giuliano reservoir, whose coordinates are shown in Table 2, satisfies half of Basilicata's irrigation needs (20 Mm^3) and the remaining half of Puglia's (20 Mm^3). The

morphology of the San Giuliano reservoir watershed slopes gradually from northwest to southeast and is characterized by different lithological formations predominant in the various sectors of the reservoir. In the western and south-western sectors, the lithology is mainly composed of clays and marls with intercalations of carbonate resediments (calcarenites, calcarenites, calcirudites) in layers and beds, numidic quartzarenites in layers and beds with intercalations of silty clays and marls, and arcosic sandstones in layers and beds with intercalations of silty clays (Mesozoic-Tertiary successions). On the other hand, the north-eastern sector of the watershed is predominantly composed of limestone (Mesozoic-Tertiary successions). In contrast, the central-eastern sector is characterized by grey-blue clays and marls and, to a lesser extent, sands, and conglomerates (Plio-Pleistocene successions).

Table 2. San Giuliano reservoir coordinates.

N-W	16°28′36.71″ E	40°37′30.18″ N
N-E	16°32′12.30″ E	40°37′30.18″ N
S-E	16°32′12.30″ E	40°35′34.03″ N
S-W	16°2836.71″ E	40°35′34.03″ N

The Mediterranean climate has hot, dry summers and mild, rainy winters. The rainfall regime is predominantly maritime, with high rainfall in late autumn and winter and low rainfall in summer. In the easternmost area, the average rainfall fluctuates around 550 mm; however, in the central part, this value increases to around 700 mm and then increases again in the westernmost part of the watershed: December is the wettest month, while August has the lowest rainfall.

The location of the reservoirs and their basins is shown in Figure 1 below.

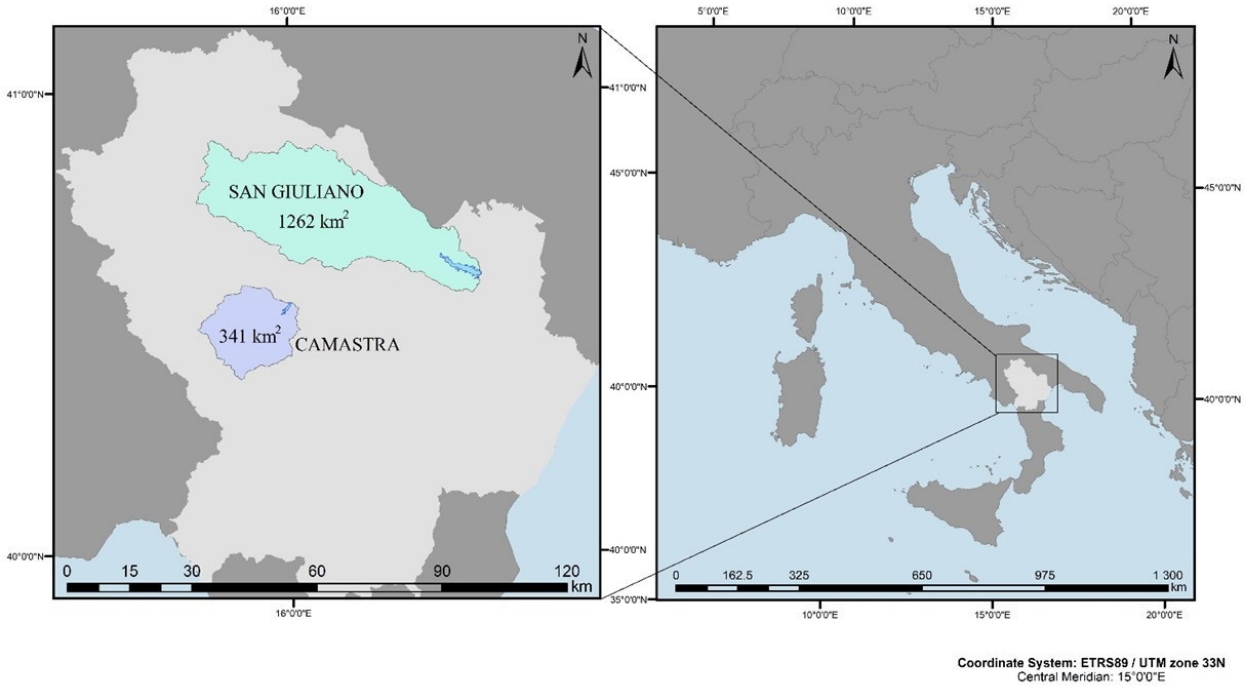

Figure 1. Study area.

2.2. Sampling Locations

Sediment samples were collected along the shores and from the bottom of the San Giuliano and the Camastra lakes in November 2021 and September 2022, respectively. Twelve surface samples and one deep sample were taken for the San Giuliano reservoir, and thirteen surface samples and four deep samples were achieved for the Camastra

reservoir, whose location was identified using GPS. The location of the sampling stations is shown in the following Figure 2.

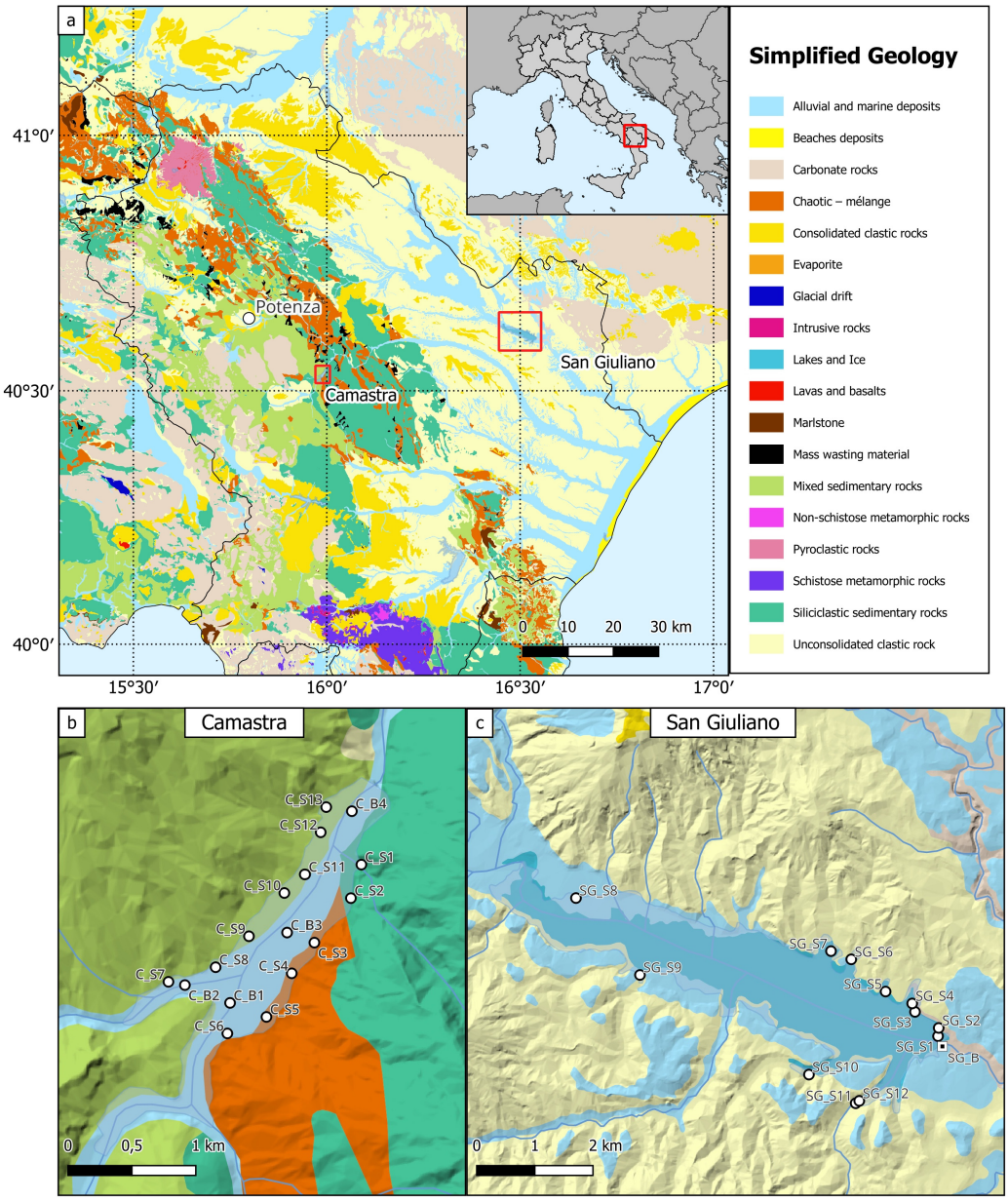

Figure 2. (**a**) Geological map of southern Italy and location of sampling points for the (**b**) Camastra and the (**c**) San Giuliano reservoirs.

The samples taken along the banks of both reservoirs are in different numbers; along the right bank of the Camastra reservoir, six samples were taken, and along the left bank, seven samples were collected. Similarly, four sites were sampled along the right bank of the San Giuliano reservoir and eight on the left bank. This discrepancy was a function of the accessibility of the various stations; the right banks of both reservoirs are less easy to reach, and even, in the case of the Camastra, it was necessary to use a boat to carry out sampling. The collecting stations were carefully chosen, favoring the areas with a more consistent presence of recently deposited sediments, to fully represent the characteristics and the degree of pollution of the upstream catchment basins (Figures 3 and 4). Due to the different geomorphological characteristics of the banks and the bottom of the reservoirs, the sediments sampled at each station have specific properties depending on their origin.

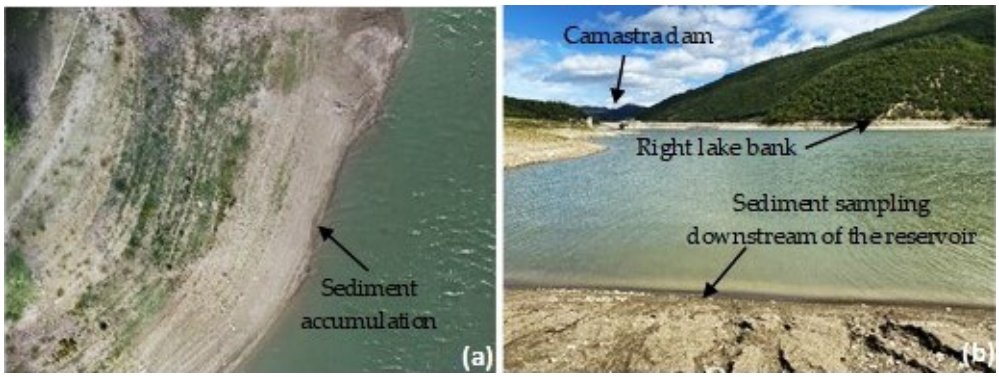

Figure 3. Sampling site of the Camastra reservoir: (**a**) top view on reservoir banks, (**b**) view near the Inferno river bridge.

Figure 4. Sampling site of the San Giuliano reservoir: (**a**) view on the right bank, (**b**) view on the left bank.

All samples were taken using portable sampling instruments made of plastic or stainless-steel materials, previously cleaned between each sampling. They were collected in glass containers, hermetically sealed at the top, labeled with the letters SG (for San Giuliano) and C (for Camastra), and identified with a number corresponding to the site where they were collected. The containers, capable of holding approximately 1 kg of collected material, appropriately labeled, were subsequently delivered to the laboratory for analysis, where they were stored at an ambient temperature of approximately 20 °C.

2.3. Sediment Characterization

To determine the main geotechnical, physic-chemical, and environmental parameters, laboratory tests were conducted on the sediments in according with national and international standards identified in Table 3.

Table 3. Standards used to test the physical, chemical, contamination, toxicology properties and parameters.

Properties or Parameters	Tests	Standards
Grain size distribution GSD	Sieving analysis	UNI EN 933-1:2012
Total organic carbon TOC	Oxidation	DM 13/09/1999 GU 248 del 21/10/1999 Method VII.3 DM 25/03/02 GU 84 del 10/04/02 Piemonte Region Compost analysis 1998 Method C 6.1
Heavy metals	Atomic Emission Spectrometry	ISO 17402:2008
Asbestos	Fourier transform infrared spectroscopy (FTIR)	D.M. 06/09/1994

The geotechnical analysis involved the determination of the leading grain size fractions, performed by sieving and evaluating the percentage passing through sieves with different diameters to identify the distribution of sandy, silty, and clayey components within each sediment sample.

To assess the pollution level of the sediments sampled at the two reservoirs, the concentration of heavy metals was determined [43,44]. The test was carried out using ICP-MS spectroscopy (mass spectrometer NexION 1000 model, manufactured by PerkinElmer Inc., based in Waltham, MA, USA, with inductively coupled plasma), which exploits the administration of relatively high energy to cause dissociation into atoms and their excitation [45]. Because of unique spectral pattern of different substances, it was possible to trace the unknown species as a function of the emitted wavelength; at the same time, the concentration of each heavy metal was calculated from the emission intensity measurement. Prior to spectrometric analyses, the digestion method used for sediment samples was the microwave mineralization, according to EPA 3051A standard, on 0.5 g of sample per sediment, to which 9 mL of HCl and 3 mL of HNO_3 were added. The temperature of each sample was increased to 175 ± 5 °C in approximately 5.5 ± 0.25 min, remaining at the same value for 4.5 min, or for the remainder of the 10-min digestion period, with subsequent cooling.

Further tests were conducted to assess the organic matter content of sediments of both reservoirs. Analyses were carried out to determine the Total Organic Carbon (*TOC*) content using the Walkley-Black method, according to Ministerial Decree 13.09.1999, based on the oxidation to carbon dioxide of the organic carbon found in the examined sample, with a solution of 0.1667 mol/L of potassium dichromate in the presence of sulphuric acid, under standardized conditions. The speed of the reaction is promoted by the rise in temperature due to the rapid dilution of the acid. In a 500 mL Erlenmeyer conical flask, 1 g of each sediment sample, air-dried and sieved to 0.5 mm, 10 mL of potassium dichromate solution and 20 mL of sulfuric acid were poured into the flask. After a set time interval of 30 min, the reaction is stopped, then adding 200 mL of distilled water, previously chilled in the refrigerator at about 4 °C. The amount of potassium dichromate that has not reacted is determined by titration with an iron (II) sulfate heptahydrate solution (0.5 mol/L). The addition of 0.5 mL of a redox indicator, the ferroin, ascertains the end of the titration. At the same time, a blank test was performed with 10 mL dichromate, 20 mL sulfuric acid and 200 mL distilled water.

For the calculation of organic carbon (*C*), expressed as a percentage, the following expression 1 was used:

$$C = 3{,}9\,\frac{(B - A)}{M} MFe\ [\%] \quad (1)$$

where *B* is the volume of iron (II) ammonium sulfate hexahydrate solution used in the titration of the blank test, expressed in ml; *A* is the volume of iron (II) ammonium sulfate hexahydrate solution used in the titration of the sample solution, expressed in ml; *MFe* is the effective molarity of the iron (II) ammonium sulfate hexahydrate solution; *M* is the mass of the soil sample, expressed in g.

Asbestos concentration for the San Giuliano and the Camastra was investigated to complete the minimal set of parameters established by the Italian Presidential Decree no. 120/2017 [46] and only for samples taken from the bottom of the reservoirs. This because, in the most depressed points, it is believed they could be affected by the highest concentrations of this parameter. In addition, a sample from the right banks of the Camastra reservoir was subjected to evaluate the possible presence of asbestos. About the latter, the sampling choice is linked to the fact that the tributary watershed of the two banks of both reservoirs is anthropized in almost the same way, the one on the right bank from the Camastra reservoir has less extension and meteorological events rapidly turn into runoff, so that a higher level of pollutants can be expected. The analytical method adopted involves the acquisition of transmittance spectra after mixing the sample with an infrared-transparent salt (KBr). Therefore, the salt was dried in an oven at 110 °C for 24 h. At the

same time, the sample, previously ground in a mill, was placed in a porcelain crucible and then in an oven at a temperature of 400 °C for one hour, to remove organic substances and kaolin. After cooling, 1.5 mg of the sample was mixed in the mill with 200 mg of KBr for 5 min. The resulting mixture was then placed in a 10-mm press and subjected to an equivalent force of 10 kN for 20 min. The material was then examined with an FTIR spectrophotometer, and acquisitions were made in wave numbers (cm^{-1}) throughout the spectral range (8000–350 cm^{-1}), achieving more excellent resolution at short wavelengths. In this way, using the software supplied with the spectrophotometer, it was possible, from the spectra acquired for each sample, to detect the concentration of asbestos in the examined sediments.

All the reagents for sample preparation are supplied by Carlo Erba Reagents, based in Milan (Italy). Instrument calibration solutions are provided by AreaChem S.r.l., based in Naples (Italy). The experimental conditions of the instrument are the following: mass-calibration with 1 µg/L solution of Be, Co, In, Ce, Pb, U; KED-calibration with Co 1 µg/L in 1% HCl. Plasma power was 1200 W, He flow was 4.6–5.2 mL/min. The instrument has a Meinhard Quartz nebuliser.

Finally, further details are provided on the laboratory tests performed for sediment characterization, fully described in the next chapter. The QA (Quality Assurance) guidelines and procedures to ensure the highest standards (QC—Quality control) were UNI EN ISO 9001:2015 and UNI EN ISO 17025:2018, respectively. Blank samples were the acids used to digest the sample treated and diluted like the real samples. They were always less than 0.1 µg/L for all parameters. The limit of detection (LoD) was calculated as three times the standard deviation obtained from 5 blank samples. In contrast, the limit of quantification (LoQ) was defined as the lowest point of the calibration line. Almost all analyzed samples showed a high metal content, and no addition (spike) tests were performed. Participation in interlaboratory circuits shows recoveries between 70% and 120%. Regarding the instrument's accuracy, it is reported that the standard deviation over three replays of the instrument's calibration solutions is less than 5%.

2.4. Data Analyses

The organic carbon content, obtained using the Walkley-Black method by Ministerial Decree 13.09.1999, and considering an average carbon content of organic substance of 580 g/kg, Equation (2) made it possible to transform the *TOC* value obtained from characterization, into organic substance, introducing a factor of 1.724 into the calculation (Tables 8 and 9). Since carbon represents, on average, 58% of the organic matter, the result of the analysis of the total organic carbon was divided by 0.58, obtaining the total organic matter (again expressed in %) through the following relationship:

$$O.M. = T.O.C. \times 1.724 \quad (2)$$

The sediment pollution degree was specified by determining the single-factor pollution index and Nemerow's integrated pollution index [40]. In particular, the combination of the two factors has been used in various research to assess heavy metal pollution [47,48]. The two indices can be calculated using Equations (3) and (4):

$$P_i = C_i / S_i \quad (3)$$

$$P_N = \left\{ \left[\left(P_{i\,avg} \right)^2 + \left(P_{i\,max} \right)^2 \right] / 2 \right\}^{1/2} \quad (4)$$

where P_i is the pollution index relative to the contaminant i, C_i is the concentration of the examined element; S_i is the reference value (Contamination Threshold Concentration, as per Italian Decree 120/2017 and column A of Table 1, Annex V, Part IV, Title V of Legislative Decree 152/06 [49]), P_N is the Nemerow integrated pollution index, $P_{i\,avg}$ is the average value of the individual pollution indices for all heavy metals, $P_{i\,max}$ is the maximum value of the individual pollution indices for all heavy metals.

The characterization data were subjected to a series of statistical tests to verify whether the sediment sampling location, characterized by specific land use and particle size distribution, could influence the content of heavy metals. The data analysis was carried out to test whether the null hypothesis (the sampling location does not influence the distribution of heavy metals) is valid for each parameter examined. The hypothesis to be tested, called the null hypothesis H_0, with which the statistical analysis of the data was started, shows that the variation in the values of most of the parameters is random; on the contrary, for some heavy metals, there is a correlation, so that it is possible to state that the alternative hypothesis H_1 is valid for them, i.e., the values found by the characterization depend on the sampling area. The level of statistical significance is expressed by a parameter called *p*-value, ranging between 0 and 1. The lower the *p*-value, the more substantial the evidence that the null hypothesis must be rejected; conventionally, a significance level of 0.05 is used. To assess whether the null hypothesis is valid or must be rejected, it is necessary to perform a test, which can be either parametric or non-parametric. The Shapiro-Wilk W test has been used to identify whether a sample has a Gaussian distribution [50–52], using Equation (5):

$$p = \frac{\left(\sum_{i=1}^{n} a_i w_{(i)}\right)^2}{\sum_{I=1}^{n}(w_i - \overline{w})^2} \quad (5)$$

where $w_{(i)}$ (index *i* included in brackets) is the smallest value of each parameter detected within the sample (order i); $\overline{w} = \frac{(w_1+\ldots+w_n)}{n}$ is the arithmetic mean of the values measured for each parameter within the examined sample; the following equation gives the constant ai (6):

$$a_i = \frac{m^T V^{-1}}{\left(m^T V^{-1} V^{-1} m\right)^{1/2}} \quad (6)$$

where $m = (m_1, \ldots, m_n)$ are the expected values of the ranks of a standardized random number, and V is the matrix of covariances of these ranks.

The next step was to check the homogeneity of the variances of the investigated samples by using a non-parametric test (Fisher's test). This test assesses whether the dichotomous data of two samples align with the null hypothesis (H_0), i.e., whether the differences observed within the sample data vectors are simply random [53]. Two tests were performed depending on the *p*-value detected for each parameter examined: the T-test, when the *p*-value was greater than 0.05, and the non-parametric Mann-Whitney test for *p*-value values less than 0.05. Both statistical tests were used to compare the averages of the considered data sets, which were independent of each other, and to check whether they differed randomly [54,55]. All the tests were performed using R software (vers. 4.0.3 for Windows), a free software environment for statistical computing and graphics. For statistical analyses, rstatix, stats, and car libraries were used (downloaded from https://cran.r-project.org/web/packages, accessed on 4 November 2023).

Analyses were carried out for heavy metals, the characterization of which provided values above the Limit of Quantification. Data was split into two vectors of six data each (for the San Giuliano reservoir) and eight and nine data each (for the Camastra reservoir), depending on the position of the sampling point, whether upstream or downstream of the reservoir. This data was subjected to statistical analysis, first through the Shapiro-Wilk test to assess the possible normal distribution of the data, and then using Fisher's test to check whether the variances were homogeneous. By using the already mentioned tests, it was thus possible to define the type of analysis, parametric or non-parametric (T-test in the first case, Mann-Whitney test in the second), that best describes the dataset and allows the validity of the null hypothesis to be assessed.

To define the possible influence of land use on the content of heavy metals and organic carbon [56], it was necessary to derive for both reservoirs, in a GIS environment, the sub-basins underlying each of the sampling stations, assumed to be the closing section. The land use characterization of all sub-basins was obtained based on the 2018 Corine Land Cover, prepared by the European Environment Agency, again through GIS analysis. The

sub-basins are characterized by 23 different land use categories, grouped into six different classes, expressed as percentages: forest, urban, non-irrigated arable land, farm areas, water bodies, and others.

3. Results and Discussion

This section describes the main experimental results achieved, their interpretation, and reports on the conclusions that can be drawn from the data analysis and their processing.

3.1. Data Focus

Table 4 shows the particle size distribution in the sediments coming from the San Giuliano reservoir. The percentages given allow us to identify a predominance of the sandy matrix in the samples coming mainly from the downstream areas of the reservoir; on the contrary, upstream samples exhibit a prominent proportion of clayey-silt particles.

Table 4. Grain size distribution of the San Giuliano sediments.

Samples	Sand > 63 μm (%)	63 μm > Silt > 2 μm (%)	Clay < 2 μm (%)
SG_S1	61.21	32.40	6.39
SG_S2	95.39	4.42	0.19
SG_S3	89.,97	4.91	5.12
SG_S4	75.90	17.47	6.63
SG_S5	34.39	32.60	33.01
SG_S6	31.35	39.59	29.06
SG_S7	48.02	38.42	13.56
SG_S8	15.51	47.56	36.93
SG_S9	23.76	49.48	26.76
SG_S10	25.85	58.25	15.90
SG_S11	4.28	61.90	33.82
SG_S12	59.27	32.19	8.54

Note: See Figure 2c for the sample's references.

Table 5 shows the percentage distribution of the different matrices in the sediments sampled at the various stations at the Camastra reservoir. The data analysis highlights what has already been observed for the materials taken from the San Giuliano reservoir. The samples collected in the downstream areas display a prevailing sandy content; those from the upstream areas of the reservoir, on the other hand, are mainly characterized by a silt-clay component. It is also noted that the sediments are, in some places, of a coarser matrix, both within the same reservoir and in comparison, with the classification of materials sampled at the San Giuliano reservoir.

Table 5. Grain size distribution of the Camastra sediments.

Samples	2 cm > Gravel > 2 mm (%)	2 mm > Sand > 63 μm (%)	63 μm > Silt > 2 μm (%)	Clay < 2 μm (%)
SG_S1	0	29.3	70.7	0
SG_S2	0	14.8	85.2	0
SG_S3	0	1.8	40.1	58.2
SG_S4	0	0.4	37.8	61.8
SG_S5	34.2	44.0	10.6	11.2
SG_S6	38.1	34.1	12.2	15.6
SG_S7	23.4	48.4	14.9	13.3
SG_S8	35.0	26.6	18.3	20.1
SG_S9	0	6.8	70.5	22.7
SG_S10	0	29.0	66.4	4.6
SG_S11	0	30.2	69.2	0.5
SG_S12	0	48.1	51.9	0

Note: See Figure 2b for the sample's references.

Tables 6 and 7 show the values of major heavy metals for the San Giuliano and Camastra reservoirs, respectively, explaining the regulatory limits set out in column A of Table 1, Annex V, Part IV, Title V of Legislative Decree 152/06, some of which are also graphically represented in Figure 5 below. As it is evident, the parameters investigated are more significant in number; nevertheless, we have presented only those with more significant findings. The remaining heavy metals investigated were not graphically displayed because the values do not show high variability compared to the mean value.

Table 6. Heavy metals concentration (mg/kg) in San Giuliano sediments (limit concentration under CTC column A, Table 1, attachment V, Italian Legislative Decree 152/06).

Heavy Metal	**Al**	**As**	**Ba**	**Be**	**Cd**	**Co**	**Cr**	**Cu**	**Fe**
LoQ	1000	1	5	0.1	0.1	1	5	5	2000
SG_B	n.a.	<1	0.022	<0.1	<0.1	7.6	24	26	n.a.
SG_S1	13,226	12	100	0.9	0.1	10	39	17	27,848
SG_S2	1288	8	30	0.2	<0.1	4	7	< 5	9487
SG_S3	2248	15	18	0.2	<0.1	4	12	6	11,067
SG_S4	4529	16	51	0.5	<0.1	9	26	11	18,732
SG_S5	12,435	**55**	82	1.0	<0.1	19	57	27	37,195
SG_S6	14,862	**31**	84	1.0	<0.1	12	57	17	30,423
SG_S7	6655	9	45	0.6	<0.1	5	25	8	14,264
SG_S8	21,151	6	81	1.5	<0.1	11	66	26	32,774
SG_S9	14,079	7	64	1.0	<0.1	10	55	19	27,365
SG_S10	9167	5	49	0.9	<0.1	8	36	16	21,712
SG_S11	16,147	7	63	1.0	<0.1	10	56	21	29,644
SG_S12	4351	5	33	0.4	<0.1	4	17	7	10,929
Limit value	n.a.	20	n.a.	2	2	20	150	120	n.a.
Heavy Metal	**Hg**	**Mn**	**Ni**	**Pb**	**Sb**	**Se**	**Tl**	**V**	**Zn**
LoQ	0.1	20	1	1	0.1	1	0.1	5	5
SG_B	<0.1	n.a.	33	16	n.a.	<1	n.a.	<5	66
SG_S1	0.1	626	34	13	0.54	1.26	0.5	76	54
SG_S2	<0.1	469	10	3	0.24	<1	<0.1	14	11
SG_S3	<0.1	314	313	4	0.29	<1	<0.1	17	15
SG_S4	<0.1	323	24	8	0.79	<1	<0.1	32	29
SG_S5	<0.1	547	59	2	0.67	<1	0.2	74	54
SG_S6	<0.1	488	50	10	0.39	<1	0.2	70	51
SG_S7	<0.1	336	21	5	0.15	<1	0.1	33	26
SG_S8	<0.1	469	47	12	0.20	<1	0.3	85	81
SG_S9	<0.1	545	46	10	0.13	<1	0.2	60	59
SG_S10	<0.1	568	30	9	0.13	<1	0.2	45	51
SG_S11	<0.1	582	39	10	0.13	<1	0.2	70	70
SG_S12	<0.1	318	15	5	0.12	<1	0.1	23	22
Limit value	1.	n.a.	120	100	10	<1	1	90	150

Note: LoQ = Limit of Quantification; n.a. = not available.

Analyses and comparisons with regulatory limits showed no exceedances for the heavy metals under investigation, except for the Arsenic value in samples SG_S5 and SG_S6, the presence of which could be related to several factors: alluvial deposits containing layers of organic matter, peat, which acts as a metals concentrator, in which arsenic contents are usually particularly conspicuous; algal organic matter in the lake environment, which also leads to the accumulation of other metals; sedimentary rocks, concentrated in the upstream area of the watershed, where it is usually significant; the use of some pesticides and herbicides, mainly used in the past; the use of phosphate and organic fertilizers; the reducing environment of the upstream area of the reservoir (as denoted by the dark-grey coloring of the sediments), which facilitates the transition from oxidation state V to oxidation state III, which is much more soluble and therefore more prone to leaching. The Arsenic content in the remaining environment is below the threshold and, therefore, of little

relevance. In any case, the overall analysis of all Arsenic values reveals that the sediment content is in line with the concentrations generally found in soils, where it ranges between 1 and 70 mg/kg [57], with an average of 10 mg/kg [58]. Concerning the sediments sampled at the Camastra reservoir, except for Cobalt in samples C_S3, C_S4, C_S8, C_S9, and C_S11, no sediments samples exceeded the regulatory limits. This metal is high in iron-magnesium minerals, common in basic and ultra-basic magmatic rocks; in contrast, it is shallow in acidic magmatic rocks. In rocks of a sedimentary nature that characterize the catchment area, the Cobalt content is also related to the origin materials [58]. Generally, the values found for all samples are in the range commonly assumed for soils worldwide, between 1 and 40 mg/kg, with an average value of about 8 mg/kg, depending on the soil-originating material. The element tends to concentrate in soil horizons rich in organic substance, showing remarkable similarity with Fe and Mn oxides, to which it binds in practically insoluble forms. In addition, the presence of Cobalt in the Camastra lake environment is linked to the presence of non-ferrous metal smelters, in which coal combustion and road traffic are less critical. However, higher values have been found in soils along high-traffic roads [57].

Table 7. Heavy metals concentration (mg/kg) in Camastra sediments (limit concentration under CTC column A, Table 1, attachment V, Italian Legislative Decree 152/06).

Heavy Metal	**Al**	**As**	**Ba**	**Be**	**Cd**	**Co**	**Cr**	**Cu**	**Fe**
LoQ	1000	1	5	0,1	0,1	1	5	5	2000
C_B1	37,581.2	4.6	119.4	1.1	0.1	12.4	54.2	30.3	39,187.6
C_B2	40,871.0	4.0	121.8	1.2	0.1	14.8	59.4	29.9	40,780.2
C_B3	48,045.8	3.8	147.2	1.6	0.1	13.4	70.0	30.3	38,313.2
C_B4	53,527.2	4.9	158.0	1.7	0.1	14.4	79.4	34.1	44,934.7
C_S1	21,926.3	8.6	199.6	0.8	0.1	9.5	34.5	20.4	29,376.4
C_S2	38,380.4	5.0	230.3	1.1	0.2	13.8	51.5	29.3	37,226.9
C_S3	34,730.2	15.6	246.2	1.2	0.1	**30.4**	67.1	36.2	48,071.5
C_S4	44,641.4	12.3	190.6	1.6	<0.1	**29.4**	58.9	41.0	59,583.3
C_S5	37,557.6	5.3	138.3	1.4	0.1	16.4	60.6	33.1	43,019.8
C_S6	34,735.1	5.0	131.4	1.1	0.1	14.5	55.4	29.9	40,824.3
C_S7	31,151.0	5.2	120.3	1.2	0.2	13.1	56.9	29.7	34,338.0
C_S8	45,757.3	13.8	130.3	1.6	<0.1	**26.0**	60.6	31.6	63,154.5
C_S9	44,455.7	9.9	163.9	1.8	0.1	**31.7**	56.1	37.4	66,448.9
C_S10	37,070.1	8.6	145.5	1.2	0.1	19.4	65.4	26.7	46,740.1
C_S11	45,483.0	5.7	134.9	1.7	0.1	**28.2**	66.0	42.8	54,386.9
C_S12	33,674.0	4.6	120.2	1.1	0.1	13.2	49.0	26.7	35,444.9
C_S13	26,931.8	6.3	111.5	0.9	0.1	14.2	44.1	24.4	34,496.8
Limit value	n.a.	20	n.a.	2	2	20	150	120	n.a.
Heavy Metal	**Hg**	**Mn**	**Ni**	**Pb**	**Sb**	**Se**	**Tl**	**V**	**Zn**
LoQ	0.1	20	1	1	0.1	1	0.1	5	5
C_B1	<0.1	902.0	35.4	10.0	0.2	1.4	0.2	59.3	73.4
C_B2	<0.1	800.6	40.4	13.6	0.2	1.6	0.3	64.7	81.1
C_B3	<0.1	751.6	43.4	12.6	0.2	2.4	0.3	76.7	82.4
C_B4	<0.1	930.6	40.7	12.8	0.2	1.8	0.3	86.7	97.1
C_S1	<0.1	834.5	28.7	11.4	0.3	<1	0.2	35.6	67.6
C_S2	<0.1	1101.5	47.1	12.1	0.3	1.4	0.2	53.6	79.8
C_S3	<0.1	1562.2	66.4	30.9	0.4	2.3	0.2	63.6	87.5
C_S4	<0.1	1067.9	52.7	18.9	0.3	2.3	0.2	60.8	106.0
C_S5	<0.1	864.8	46.7	14.6	0.3	2.4	0.2	65.4	87.1
C_S6	<0.1	968.0	35.0	10.4	0.2	1.5	0.2	61.4	77.3

Note: LoQ = Limit of Quantification; n.a. = not available.

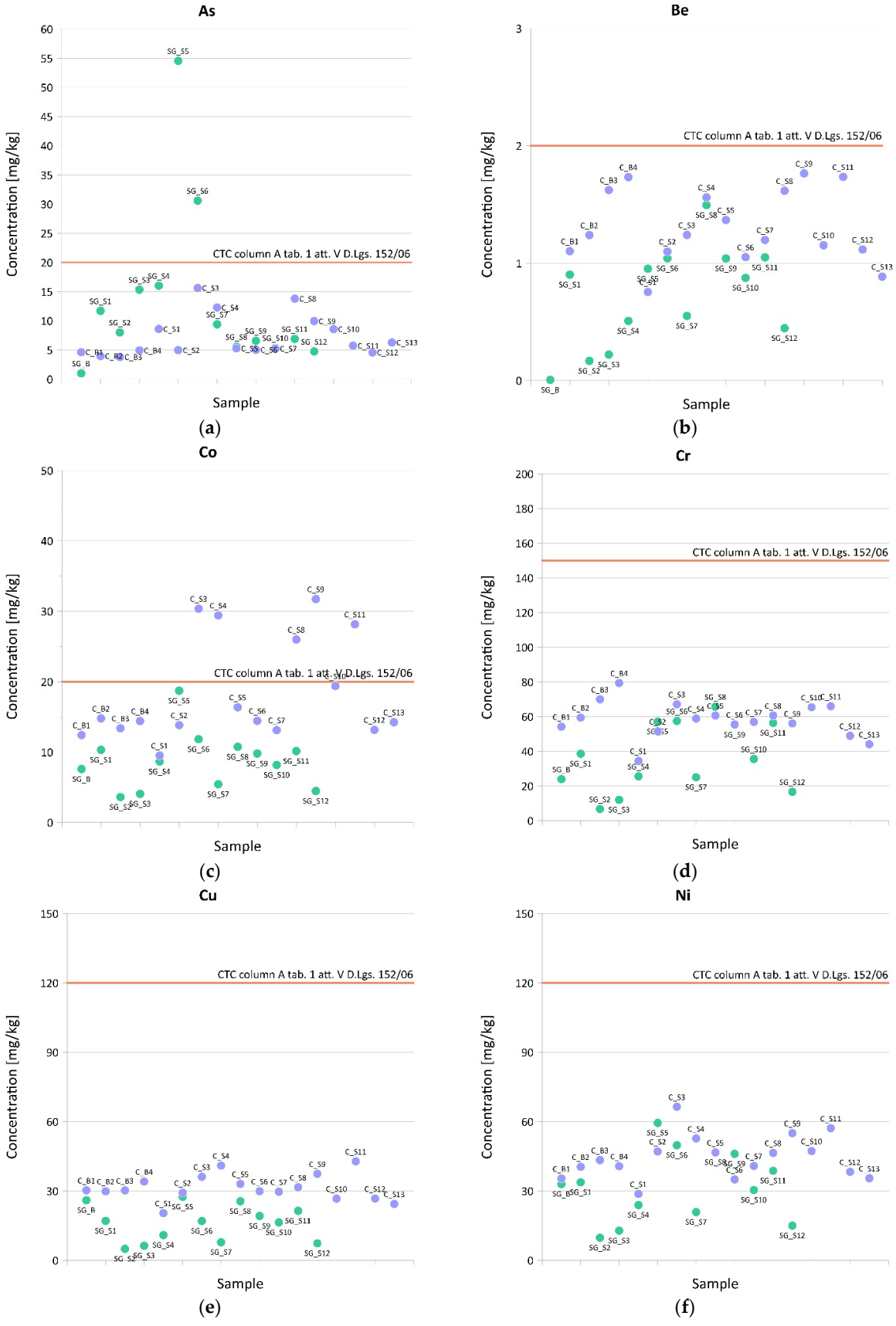

Figure 5. *Cont.*

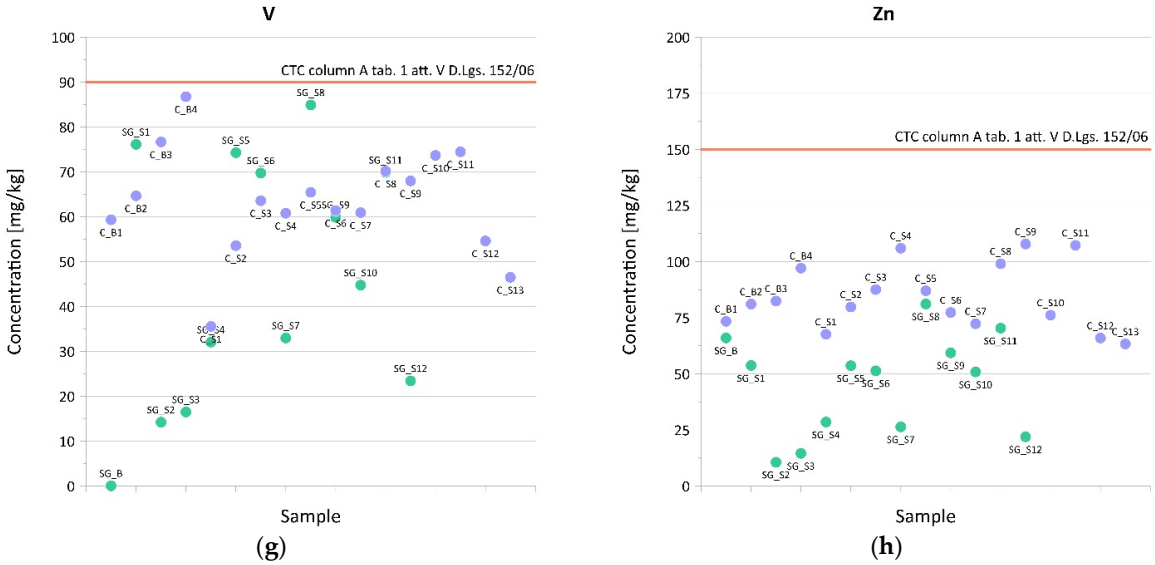

Figure 5. Values of (**a**) Arsenic, (**b**) Beryllium, (**c**) Cobalt, (**d**) Chromium, (**e**) Copper, (**f**) Nickel, (**g**) Vanadium, and (**h**) Zinc detected in each sediment sample of the San Giuliano and the Camastra reservoirs, with the Contamination Threshold Concentration (Presidential Decree 120/2017 and Legislative Decree 152/2006), where "SG" code stands for San Giuliano (green dots) and "C" code stands for Camastra (purple dots).

Tables 8 and 9 define the measured values for Total Organic Carbon (TOC) and Organic Matter in the sediments sampled from both reservoirs under study.

The measurements show a higher content of both parameters for the Camastra sediments than those of San Giuliano. For the latter, the percentages of the detected organic matter are below 2%, considered the organic matter content below which soil must not ensure its nutritional and structural functions and guarantee adequate fertility. The Camastra's surface sediments also have organic matter percentages of less than 2%; in contrast, for the deep samples, the values are above 2%, so the latter can guarantee ecosystem functions for plant species. However, for the overall reuse of the Camastra sediments, the average organic matter content is less than 2%, resulting in a situation similar to that of the San Giuliano reservoir (Figure 6).

Table 8. Carbon properties of San Giuliano sediments.

Sample	Total Organic Carbon TOC (%)	Organic Matter OM (%)
SG_S1	0.54	0.93
SG_S2	0.35	0.61
SG_S3	0.03	0.05
SG_S4	0.17	0.29
SG_S5	1.02	1.76
SG_S6	0.36	0.61
SG_S7	0.25	0.43
SG_S8	0.34	0.58
SG_S9	0.54	0.93
SG_S10	0.81	1.40
SG_S11	0.05	0.09
SG_S12	0.14	0.24
SG_S1	0.54	0.93

Table 9. Carbon properties of Camastra sediments.

Sample	Total Organic Carbon TOC (%)	Organic Matter OM (%)
C_B1	1.45	2.50
C_B2	1.69	2.91
C_B3	1.32	2.28
C_B4	0.85	1.47
C_S1	0.77	1.33
C_S2	0.88	1.52
C_S3	0.69	1.19
C_S4	1.00	1.72
C_S5	1.02	1.76
C_S6	0.85	1.47
C_S7	0.68	1.17
C_S8	0.70	1.21
C_S9	0.82	1.41
C_S10	0.62	1.07
C_S11	0.73	1.26
C_S12	0.80	1.38
C_S13	0.66	1.14

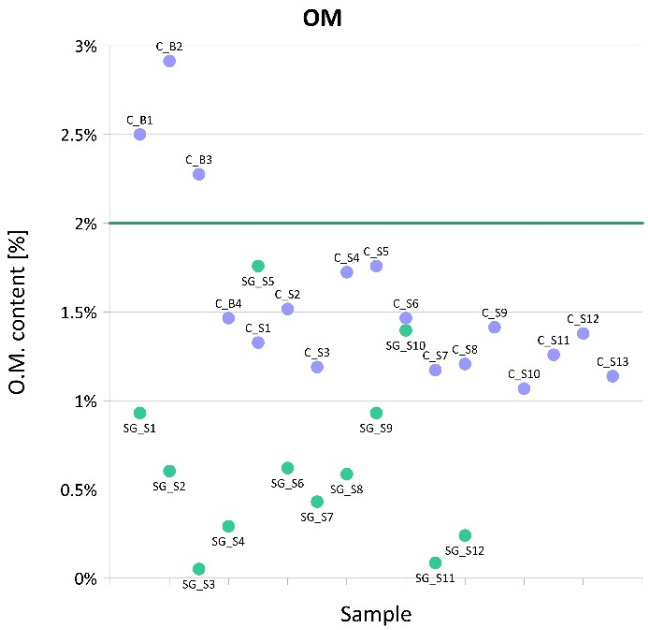

Figure 6. Organic matter content measured in each sediment sample of the San Giuliano and the Camastra reservoirs, with an indication of the recommended organic matter content above which adequate fertility is guaranteed (threshold 2%), where "SG" code stands for San Giuliano (green dots) and "C" code stands for Camastra (purple dots).

Finally, Table 10 shows the asbestos concentrations in some samples collected at the Camastra and San Giuliano reservoirs.

Table 10. Asbestos concentration (mg/kg) of the bottom San Giuliano sample and the bottom and surface Camastra samples (limit of concentration pursuant to CTC column A, Table 1, attachment V, Italian Legislative Decree 152/06).

Other Parameters	LoQ	SG_B	C_B1	C_B3	C_S3	Limit Value
Asbestos	500	<500	<500	<500	<500	1000

The laboratory analysis results show that the presence of this element in all the samples analyzed is always below 500 mg/kg (guaranteeing the absence of asbestos fibers), below the limit established in column A, Table 1, Annex 5, Part Four, Title V, of Legislative Decree 152/2006.

3.2. Correlation between the Analyzed Parameters

As pointed out in previous research, some of the parameters investigated may be related to each other, and their values may be a function of the characteristics of the sampling site. For example, a correlation was found between the concentration of all or some of the heavy metals detected and the grain size distribution function of the point of origin of the sampled material [32]. Therefore, based on this hypothesis, the present study investigates, using statistical tests, whether the values of the detected heavy metals can be related to the characteristics of the sampling station, especially grain size distribution and land use.

Since the analyses carried out with the Shapiro-Wilk test have shown a normal distribution of the data, Fisher's test was used to verify the homogeneity of the variances, obtaining both homogeneous and non-homogeneous sample variances. Therefore, it became necessary to use two different tests to check if the null hypothesis could be rejected, i.e., the Student T-test and the Mann-Whitney test.

From the analyses carried out, it emerges that, concerning the sediments from the San Giuliano reservoir (Table 11), the Shapiro-Wilk test returned a p-value greater than 0.05. Therefore, it is possible to accept the null hypothesis, according to which the data follow a normal distribution. Subsequently, the application of Fisher's test to both data vectors shows that the p-value is more significant than 0.05 (variances are homogeneous), except for Arsenic. Therefore, for all parameters, Student's T-test was performed; in contrast, for Arsenic alone, the non-parametric Mann-Whitney test was used, to compare the averages of two groups of samples extracted from two populations with homogeneous or non-homogeneous sample variances.

In this study, the null hypothesis H_0 to be tested is that the distribution of heavy metals is not influenced by the sampling position within the catchment area; since this is considered acceptable as the p-value $p > 0.05$, it can be said to be verified for most parameters. This is not true, however, for Be, Cr and Ni ($p < 0.05$, in red), for which it is necessary to accept the alternative hypothesis H_1, i.e., the concentration of these elements is influenced by the sampling point and site characteristics.

For the sediments sampled at the Camastra reservoir, the statistical analyses (Table 12) results show that the data follow a normal distribution (the null hypothesis is verified) since the p-value obtained from the Shapiro-Wilk test is more significant than 0.05. Fisher's test, on the other hand, shows that, for most of the parameters considered, the variances are homogeneous (p-value > 0.05), and for these, the Student's T-test was performed. For Chromium, Thallium, and Vanadium only, the p-value resulting from Fisher's test is less than 0.05; for these parameters, the non-parametric Mann-Whitney test was used to check the acceptability or otherwise of the null hypothesis.

The analysis of the data in Table 12 shows that for all parameters, the null hypothesis H_0 can be accepted (the position within the catchment area does not influence the distribution of heavy metals); therefore, for the Camastra sediments, the concentration of these elements is not influenced by the sampling point and site characteristics.

Table 11. Test results for heavy metals of the San Giuliano reservoir.

		Shapiro—Wilk Test	Fisher Test	T-Test	Mann-Whitney Test
Aluminum (Al)	*p*-value upstream samples	0.8864	0.6621	0.09037	-
	p-value downstream samples	0.128			
Arsenic (As)	*p*-value upstream samples	0.02253	0.004996	-	1
	p-value downstream samples	0.5165			
Barium (Ba)	*p*-value upstream samples	0.1354	0.2719	0.2205	-
	p-value downstream samples	0.5276			
Beryllium (Be)	*p*-value upstream samples	0.2535	0.7138	**0.02941**	-
	p-value downstream samples	0.2384			
Cobalt (Co)	*p*-value upstream samples	0.6676	0.3893	0.1136	-
	p-value downstream samples	0.01355			
Chromium (Cr)	*p*-value upstream samples	0.2625	0.7067	**0.04032**	-
	p-value downstream samples	0.5937			
Copper (Cu)	*p*-value upstream samples	0.6274	0.8748	0.07862	-
	p-value downstream samples	0.2954			
Iron (Fe)	*p*-value upstream samples	0.8858	0.8671	0.08686	-
	p-value downstream samples	0.1382			
Manganese (Mn)	*p*-value upstream samples	0.1568	0.2926	0.4462	-
	p-value downstream samples	0.101			
Nickel (Ni)	*p*-value upstream samples	0.5631	0.7326	**0.02553**	-
	p-value downstream samples	0.4024			
Lead (Pb)	*p*-value upstream samples	0.1532	0.4118	0.17	-
	p-value downstream samples	0.6442			
Antimony (Sb)	*p*-value upstream samples	0.03497	0.6717	0.6092	-
	p-value downstream samples	0.2405			
Thallium (Tl)	*p*-value upstream samples	0.101	0.06233	0.8174	-
	p-value downstream samples	0.001158			
Vanadium (V)	*p*-value upstream samples	0.8618	0.4634	0.1309	-
	p-value downstream samples	0.09543			
Zinc (Zn)	*p*-value upstream samples	0.5218	0.546	0.1233	-
	p-value downstream samples	0.3177			

3.3. Influence of Grain Size Distribution, Land Use, and Total Organic Carbon on Heavy Metal Content

The accumulation of heavy metals in sediments can be influenced by two main factors: grain size distribution and organic carbon content [33]. The organic carbon content of all the samples analyzed is 0.03% to 1.69%, with an average value of 0.91% for the Camastra reservoir sediments and 0.38% for those from San Giuliano. The most organic carbon is found in the sediments taken from the bottom of the Camastra reservoir, i.e., those mainly characterized by fine particle-size components. However, the organic carbon content is not closely related to the clay or sandy fraction (the regression coefficient is 0.31 and 0.36, respectively), suggesting that the organic matter content in sediments is not controlled by grain size distribution. Therefore, the organic carbon values found are probably related to local factors, such as erosion of rocks and soils rich in organic matter.

Table 12. Test results for heavy metals of the Camastra reservoir.

		Shapiro—Wilk Test	Fisher Test	T-Test	Mann-Whitney Test
Aluminum (Al)	*p*-value upstream samples	0.5267	0.1024	0.6493	-
	p-value downstream samples	0.9583			
Arsenic (As)	*p*-value upstream samples	0.03407	0.06005	0.3156	-
	p-value downstream samples	0.1679			
Barium (Ba)	*p*-value upstream samples	0.03223	0.1085	0.1868	-
	p-value downstream samples	0.2368			
Beryllium (Be)	*p*-value upstream samples	0.5786	0.3991	0.5124	-
	p-value downstream samples	0.298			
Cobalt (Co)	*p*-value upstream samples	0.05893	0.7311	0.5215	-
	p-value downstream samples	0.01628			
Chromium (Cr)	*p*-value upstream samples	0.4834	0.0002189	-	0.8944
	p-value downstream samples	0.6628			
Copper (Cu)	*p*-value upstream samples	0.0148	0.1904	0.3183	-
	p-value downstream samples	0.8995			
Iron (Fe)	*p*-value upstream samples	0.08483	0.2291	0.1604	-
	p-value downstream samples	0.8223			
Manganese (Mn)	*p*-value upstream samples	0.3145	0.5804	0.5712	-
	p-value downstream samples	0.04421			
Nickel (Ni)	*p*-value upstream samples	0.488	0.3111	0.8715	-
	p-value downstream samples	0.8075			
Lead (Pb)	*p*-value upstream samples	0.3724	0.2038	0.6291	-
	p-value downstream samples	0.01533			
Antimony (Sb)	*p*-value upstream samples	0.5021	0.393	0.2853	-
	p-value downstream samples	0.4418			
Thallium (Tl)	*p*-value upstream samples	0.2443	0.01631	-	0.9778
	p-value downstream samples	0.1311			
Vanadium (V)	*p*-value upstream samples	0.3514	0.00107	-	0.9159
	p-value downstream samples	0.8593			
Zinc (Zn)	*p*-value upstream samples	0.2134	0.9959	0.3348	-
	p-value downstream samples	0.69			

The materials sampled at the Camastra and San Giuliano reservoirs are mainly characterized by sandy fractions downstream and by silt-clay fractions upstream. In the samples taken in the reservoir areas closest to the dams, the sand content is consistently above 50%, averaging 64.3% ± 32.9%. In the case of the Camastra, percentages of sandy components in the downstream samples reached around 70%. However, a part of this percentage is represented by the fraction with a diameter between 2 mm and 2 cm (Figures 7 and 8), except for the areas close to the dams. In the upstream areas, on the other hand, the silt-clay fraction is prevalent, averaging around 65% ± 14.3%. Finally, the grain size distribution of the deep samples shows a low presence of the sandy component, and in one sample (sample C_B4), it is completely absent. In any case, data shown in Tables 4 and 5 and Figures 7 and 8 highlight that the particle size composition of all samples crosses several fractions. Therefore, it can be stated that the sediments are poorly graded.

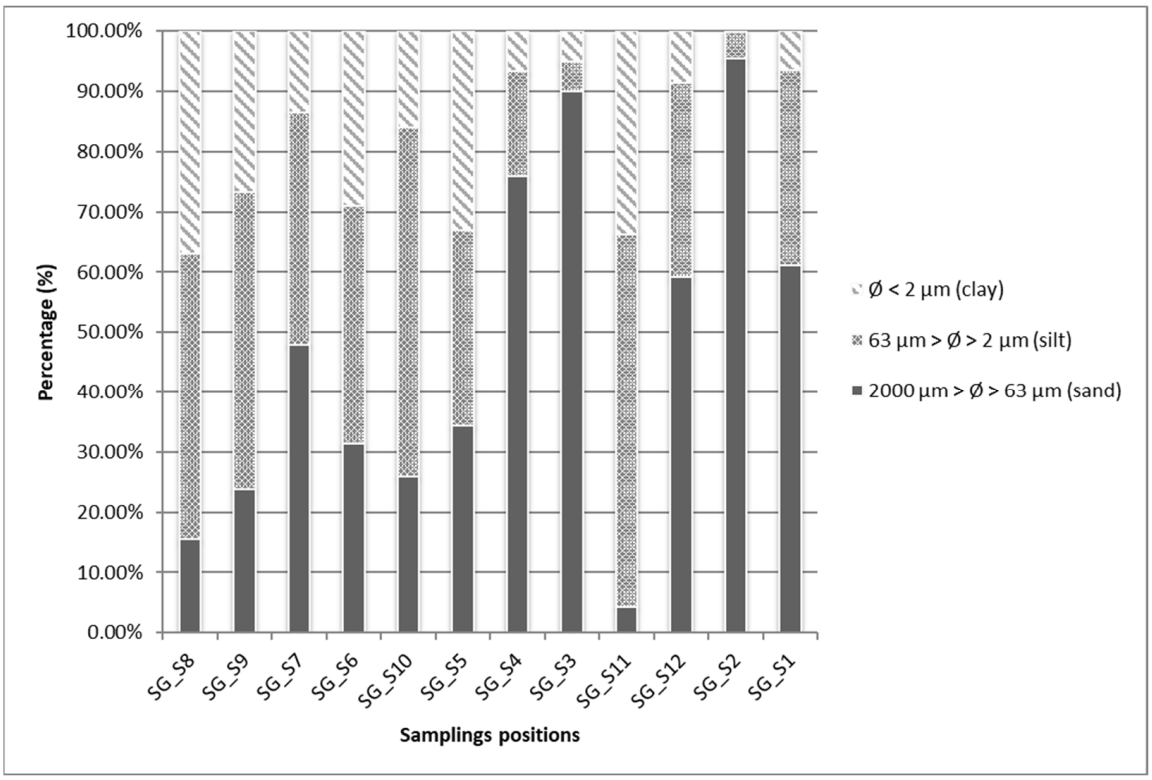

Figure 7. Distribution of grain size composition of the San Giuliano sediments (from upstream to downstream), where "SG" code stands for San Giuliano.

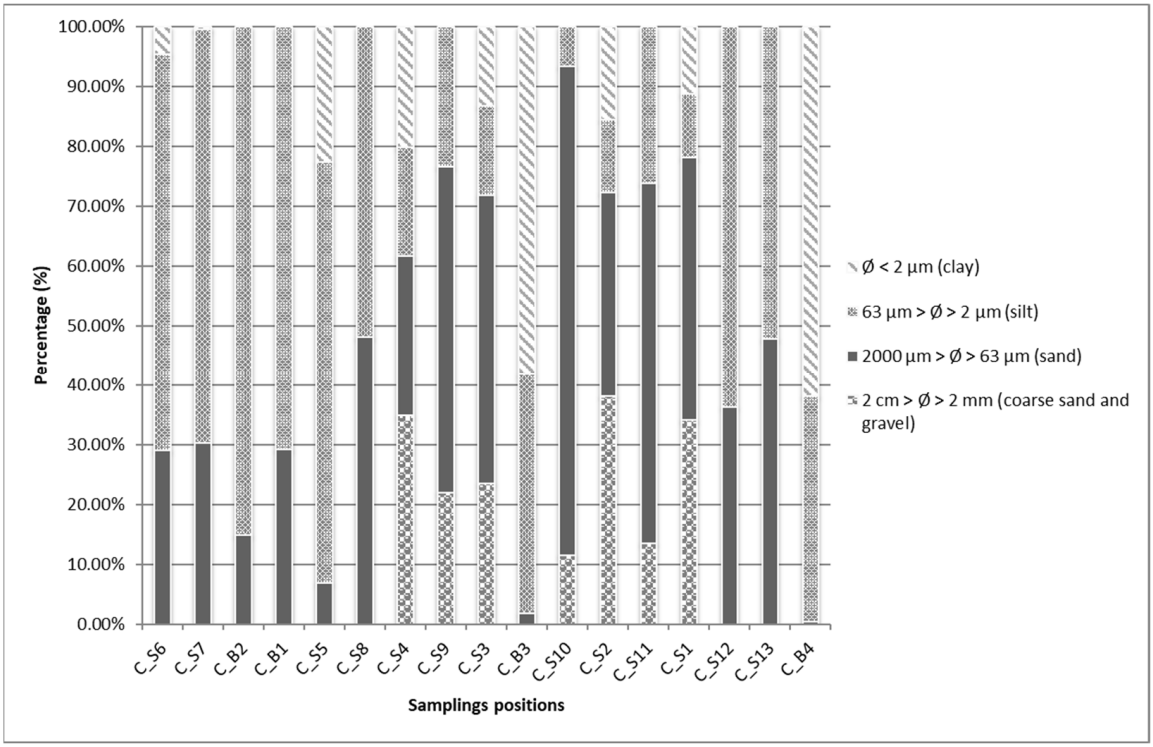

Figure 8. Distribution of grain size composition of the Camastra sediments (from upstream to downstream), where "C" code stands for Camastra.

Land use is one of the main factors governing the accumulation of heavy metals in sediments; indeed, previous research has shown that their increase is related to predominantly urban land use [35,59,60]. In the examined scenario, regarding the correlation between land use and the presence of heavy metals in the analyzed sampling points, the distribution of land use was evaluated for each sub-basin subtended by the closure section represented by each sampling point. For the San Giuliano reservoir (Table 13), almost all the area of each sub-basin is characterized by a land use referred to as 'non-irrigated arable land,' for an average percentage of 95%, which reaches 99% in the case of the sub-basin subtended by sampling station SG_S11. Other land-use categories are limited to small percentages and irrelevant to the assessments. Similarly, in the case of the Camastra reservoir (Table 14), land use is predominantly characterized by 'forest', which in the sub-basins covers an area of between 20% and 100% of the total surface area, and by 'non-irrigated arable land,' which is not present everywhere, with percentages averaging 20%. Urban-type land use is only found in the sub-basins belonging to the closure sections C_B1, C_B3, and C_B4, although the percentage of total area covered is less than 1%. On average, although only in some sub-basins considered, agricultural areas currently cover 15% of the total area are essential.

Table 13. Land use percentage of the sub-basin for each San Giuliano reservoir sampling site.

Sample	Forest %	Urban %	Non-Irrigated Arable Land %	Farm Areas %	Water Bodies %	Other Areas %
SG_S1	3.45	0.12	94.88	0.41	1.02	0.12
SG_S2	3.45	0.12	94.88	0.41	1.02	0.12
SG_S3	3.41	0.19	94.99	0.27	1.03	0.12
SG_S4	3.41	0.19	94.99	0.27	1.03	0.12
SG_S5	3.41	0.19	94.99	0.27	1.03	0.12
SG_S6	3.38	0.19	95.01	0.27	1.03	0.12
SG_S7	3.38	0.19	95.01	0.27	1.03	0.12
SG_S8	3.41	0.19	95.83	0.28	0.17	0.12
SG_S9	3.38	0.15	95.04	0.27	1.03	0.12
SG_S10	3.45	0.12	94.88	0.41	1.02	0.12
SG_S11	0.22	0.01	99.47	0.30	0.00	0.00
SG_S12	3.40	0.12	94.93	0.41	0.00	0.12

Table 14. Land use percentage of the sub-basin for each Camastra reservoir sampling site.

Sample	Forest %	Urban %	Non-Irrigated Arable Land %	Farm Areas %	Water Bodies %	Other Areas %
C_B1	64.88	0.41	19.14	14.97	0.57	0.00
C_B2	98.22	0.00	0.00	0.00	1.77	0.00
C_B3	64.81	0.41	19.13	14.93	0.70	0.00
C_B4	64.90	0.40	19.02	14.79	0.87	0.00
C_S1	81.32	0.00	18.67	0.00	0.00	0.00
C_S2	97.66	0.00	2.33	0.00	0.00	0.00
C_S3	78.06	0.00	19.46	2.47	0.01	0.00
C_S4	89.31	0.00	0.00	10.26	0.42	0.00
C_S5	99.99	0.00	0.00	0.00	0.00	0.00
C_S6	43.79	0.00	44.83	10.01	1.34	0.00
C_S7	89.44	0.00	0.00	0.00	10.55	0.00
C_S8	100.00	0.00	0.00	0.00	0.00	0.00
C_S9	63.83	0.00	18.37	17.78	0.00	0.00
C_S10	66.58	0.00	33.38	0.00	0.02	0.00
C_S11	19.71	0.00	79.63	0.00	0.65	0.00
C_S12	80.77	0.00	6.93	0.00	12.28	0.00
C_S13	89.25	0.00	10.74	0.00	0.00	0.00

It is well known that the heavy metal content in soils is significantly influenced by both the natural background concentration, related to the type of rocks in place, and the anthropogenic activities taking place within the catchment area. The latter include industrial activities, mining and smelting activities, fertilization of soils with nutrients and agronomic products, wastewater irrigation, sludge disposal on the ground, and vehicle demolition activities [61]. The findings of the analyses reveals that anthropogenic activities scarcely characterize the land use of both watersheds. Consequently, the content of heavy metals in sediments is insignificant, and the threshold values set by Italian regulations are not exceeded.

3.4. Pollution Assessment

The results of the assessment of the single pollution index (P_i) and the Nemerow integrated pollution index (P_N) are shown in Table 15 and Figure 9 for the San Giuliano reservoir and Table 16 and Figure 10 for the San Giuliano reservoir.

Table 15. Single pollution index (P_i) of San Giuliano sediments.

	As	Be	Co	Cr	Cu	Ni	Pb	Sb	Tl	V	Zn
SG_B	0.050	0.003	0.380	0.160	0.217	0.275	0.160	n.a.	n.a.	0.001	0.440
SG_S1	0.585	0.451	0.516	0.257	0.142	0.281	0.126	0.054	0.515	0.846	0.358
SG_S2	0.400	0.084	0.181	0.045	0.042	0.081	0.030	0.024	0.100	0.158	0.071
SG_S3	0.767	0.110	0.204	0.080	0.053	0.107	0.041	0.029	0.100	0.183	0.097
SG_S4	0.801	0.254	0.433	0.171	0.091	0.200	0.080	0.079	0.100	0.356	0.190
SG_S5	2.727	0.476	0.936	0.381	0.229	0.495	0.224	0.067	0.228	0.825	0.358
SG_S6	1.530	0.521	0.592	0.383	0.142	0.415	0.099	0.039	0.241	0.775	0.342
SG_S7	0.470	0.276	0.272	0.167	0.065	0.174	0.052	0.015	0.144	0.367	0.176
SG_S8	0.278	0.748	0.537	0.439	0.213	0.390	0.118	0.020	0.307	0.943	0.541
SG_S9	0.329	0.520	0.490	0.368	0.160	0.384	0.095	0.013	0.217	0.665	0.396
SG_S10	0.268	0.438	0.409	0.237	0.137	0.254	0.086	0.013	0.189	0.497	0.339
SG_S11	0.345	0.525	0.507	0.376	0.178	0.323	0.097	0.013	0.214	0.776	0.469
SG_S12	0.237	0.223	0.224	0.111	0.061	0.125	0.052	0.012	0.120	0.260	0.146

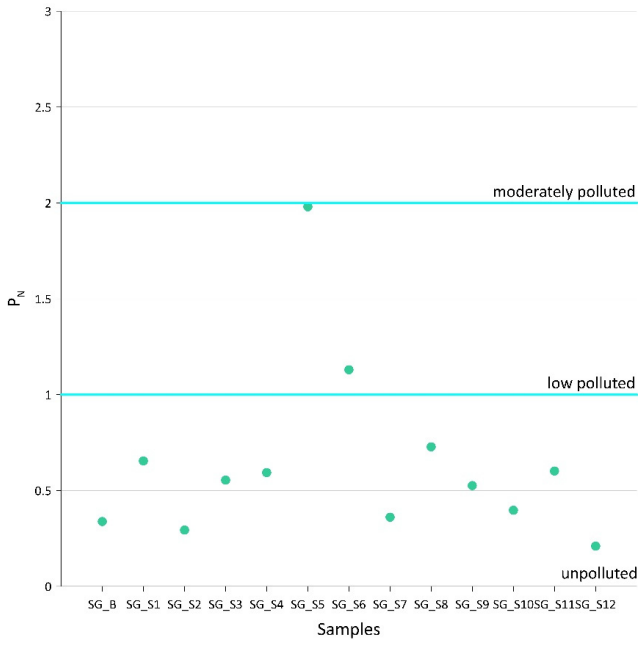

Figure 9. Nemerow integrated pollution index (P_N) of heavy metal of San Giuliano sediments, where "SG" code stands for San Giuliano (green dots).

Table 16. Single pollution index (P_i) of Camastra sediments.

	As	Be	Co	Cr	Cu	Ni	Pb	Sb	Tl	V	Zn
C_B1	0.231	0.551	0.621	0.361	0.253	0.295	0.100	0.020	0.207	0.659	0.489
C_B2	0.198	0.619	0.739	0.396	0.249	0.337	0.136	0.020	0.253	0.719	0.541
C_B3	0.190	0.812	0.669	0.467	0.252	0.361	0.126	0.023	0.318	0.852	0.550
C_B4	0.246	0.867	0.721	0.529	0.284	0.339	0.128	0.023	0.296	0.964	0.647
C_S1	0.430	0.377	0.476	0.230	0.170	0.239	0.114	0.026	0.172	0.395	0.451
C_S2	0.248	0.549	0.691	0.343	0.244	0.393	0.121	0.032	0.213	0.595	0.532
C_S3	0.781	0.620	1.518	0.448	0.301	0.554	0.309	0.038	0.195	0.706	0.584
C_S4	0.613	0.781	1.471	0.393	0.342	0.439	0.189	0.028	0.226	0.675	0.707
C_S5	0.263	0.684	0.818	0.404	0.276	0.389	0.146	0.025	0.240	0.727	0.580
C_S6	0.252	0.526	0.723	0.370	0.249	0.292	0.104	0.021	0.202	0.682	0.516
C_S7	0.262	0.599	0.656	0.379	0.247	0.340	0.114	0.023	0.238	0.677	0.482
C_S8	0.690	0.808	1.299	0.404	0.263	0.387	0.163	0.026	0.201	0.780	0.660
C_S9	0.497	0.882	1.586	0.374	0.312	0.459	0.204	0.031	0.233	0.756	0.719
C_S10	0.429	0.577	0.969	0.436	0.223	0.394	0.186	0.029	0.198	0.818	0.507
C_S11	0.286	0.868	1.408	0.440	0.357	0.476	0.171	0.028	0.226	0.828	0.715
C_S12	0.229	0.558	0.658	0.326	0.223	0.319	0.104	0.020	0.233	0.607	0.440
C_S13	0.314	0.442	0.712	0.294	0.203	0.296	0.145	0.023	0.175	0.517	0.422

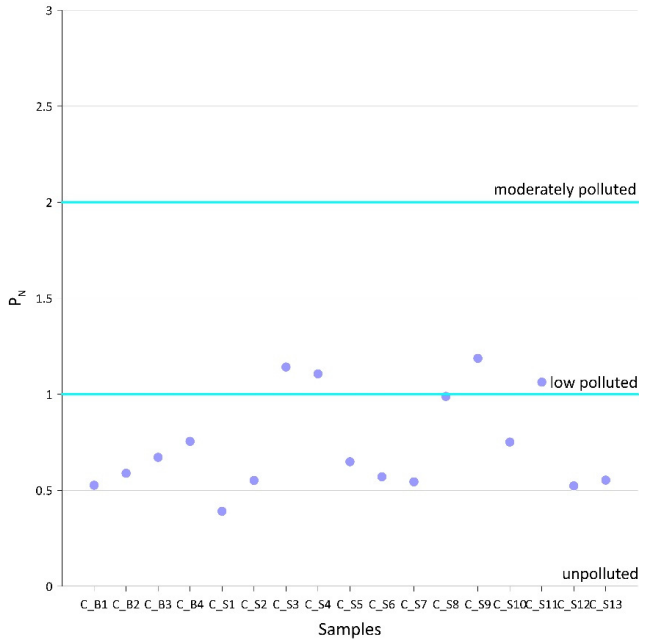

Figure 10. Nemerow integrated pollution index (P_N) of heavy metal of Camastra sediments, where "C" code stands for Camastra (purple dots).

Regarding the San Giuliano reservoir, the Pi index shows that for all heavy metals and all sediments, the values are always less than 1, indicating a non-polluted condition of the sediments. An exception concerns the sediments SG_S5 and SG_S6, for which P_i index values for Arsenic are between 2 and 3 and between 1 and 2, respectively. Therefore, it is possible to define that sediment SG_S5, regarding Arsenic, is moderately polluted, whereas sediment SG_S6 is low polluted.

The Nemerow integrated pollution index P_N illustrates a similar condition to the one found above. All sediments, except SG_S5 and SG_S6, can be defined unpolluted, with values well below unity. In contrast, the sediments mentioned above have a P_N value between 1 and 2, i.e., they are, on the whole, low-polluted. However, the P_N index of sediment SG_S5 is close to 2, tending towards a moderately polluted condition.

In the case of the Camastra sediments, the P_i index is always less than unity for all the parameters examined, and all the sediments sampled, indicating an unpolluted condition. For samples C_S3, C_S4, C_S8, C_S9, and C_S11, the single pollution index for Cobalt is between 1 and 2, indicating a low-pollution condition.

However, Figure 10 shows that most of the sediments are unpolluted, except for samples C_S3, C_S4, C_S9, and C_S11, which are low polluted. In contrast to the single pollution index, therefore, overall, for sample C_S8, there is no polluted condition, although the P_N value is very close to unity (0.989); on the contrary, the sediments above slightly exceed the unity, settling at a value of about 1.1, indicating a low polluted condition.

Overall, the findings of the analyses show that the heavy metal content is below the limit values fixed by the Italian Regulations, assumed to be the standards for sediment reuse. In other words, the sediment is substantially compatible, without prior treatment, for reuse in environmental recovery (as filling material for disused quarries, earth embankments, and dykes, reprofiling of riverbed morphometry, nourishment of shorelines and sandy shores, reconstruction of coastal morphologies) and for the construction of embankments and sub-bases, moving the dredged material outside the area of operation as by-products, by the compliance mentioned above with regulatory limits. Furthermore, considering that plants' uptake of Arsenic and Cobalt is not high, nor are there any potentially harmful effects for humans, it is also possible to hypothesize reuse in the agronomic field as inorganic fertilizer due to the low organic content. In conclusion, this research on the Camastra and San Giuliano reservoir sediments is the first step towards identifying potential alternative reuses to landfill disposal. In this regard, some research has already been started, mainly to verify the compatibility of sediments for reuse as aggregate and binder in the preparation of cement mortars, with preliminary evidence that was very encouraging [62].

4. Conclusions

The reduction in the storage capacity of the reservoirs, related to the significant inflow of sediments, requires the initiation of dredging operations and the subsequent management of these materials, now labeled by legislation as waste [63]. To recover and reuse them for other uses, it is essential to perform characterization activities, which help define the specific properties of sediments and to identify the possible reuses. The present study analyzed the results of analyses on sediments sampled at the San Giuliano and Camastra reservoirs in southern Italy to verify their suitability for reuse.

Tests showed that the downstream sediments of the reservoirs have a predominantly sandy grain size composition while upstream sediments have a mostly silt-clay composition. The absence of heavy metal pollution is observed, as the values obtained from the laboratory analyses, compared with the primary legislative references, are well below the regulatory limits, with a few exceptions. Some of the samples from the Camastra reservoir exceed the threshold values for Cobalt alone; on the contrary, for the San Giuliano reservoir, Arsenic exceeds the limits, again in a small number of sampling points. The assessment by determining the P_i and P_N pollution indices reinforces the aforementioned conclusion, allowing the sediments to be classified in the 'unpolluted' and 'low polluted' categories. The organic matter content was low in most of the samples analyzed; the highest content, over 2%, was found exclusively in sediments from the bottom of the Camastra reservoir. Similarly, laboratory tests showed the total absence of asbestos.

Another conclusion reached is the absence of correlation between the sampling point and the heavy metal content of the sediments, except for the Be, Cr and Ni parameters in those of the San Giuliano reservoir. This is probably related to the different land use of the San Giuliano basin compared to that of the Camastra one, which is more anthropized by agricultural activities, also because, in both, the presence of urban areas, another factor influencing the heavy metal content, is of little relevance. Therefore, the potential cause of the correlation between land use and the content of Be, Cr and Ni in the sediments is hypothesized to be the extensive farming activity carried out in the San Giuliano watershed, and particularly the use of fertilizers composed of the previously mentioned metals, such

as to govern their distribution in the sampled materials. On the other hand, no correlation was found between heavy metal content and organic carbon content. The same can be said about grain size composition. Therefore, organic carbon and grain size distribution cannot be counted among the main factors governing the distribution of heavy metals in sediments.

Author Contributions: Paper conceptualization, D.L.; methodology, D.L.; data providing, T.T.; software elaboration, A.M.N.M.; formal analysis, A.M.N.M.; writing-original draft preparation, A.M.N.M.; writing-review and editing, D.L. and A.F.P.; validation, G.R. and F.G.; supervision, A.F.P. and F.G.; project management and administration, A.F.P. and F.G. All authors have read and agreed to the published version of the manuscript.

Funding: This research received no external funding.

Institutional Review Board Statement: Not applicable.

Informed Consent Statement: Not applicable.

Data Availability Statement: The data supporting this study's findings are available from the corresponding author upon request due to privacy.

Acknowledgments: The authors would like to express their thanks and gratitude to the Ente per lo Sviluppo dell'Irrigazione e la Trasformazione Fondiaria in Puglia, Lucania e Irpinia (E.I.P.L.I.) and to the Consorzio di Bonifica della Basilicata for their collaboration and technical support. Additionally, the authors wish to acknowledge Xavier Pellerin Le Bas, PostDoc researcher at the laboratory "Morphodynamique Continentale et Côtière -M2C" of the University of Caen Normandie for providing help in the elaboration of the geological map.

Conflicts of Interest: The authors declare no conflict of interests.

References

1. de Araújo, J.C.; Güntner, A.; Bronstert, A. Loss of reservoir volume by sediment deposition and its impact on water availability in semiarid Brazil. *Hydrol. Sci. J.* **2006**, *51*, 157–170. [CrossRef]
2. Khagram, S. *Dams and Development*; Cornell University Press: Ithaca, NY, USA, 2018. [CrossRef]
3. Niu, Y.; Shah, F.A. Economics of optimal reservoir capacity determination, sediment management, and dam decommissioning. *Water Resour. Res.* **2021**, *57*, e2020WR028198. [CrossRef]
4. Canlı, O.; Çetintürk, K.; Güzel, B. A comprehensive assessment, source input determination and distribution of persistent organic pollutants (POPs) along with heavy metals (HMs) in reservoir lake sediments from Çanakkale province, Türkiye. *Environ. Geochem. Health* **2023**, *45*, 3985–4006. [CrossRef] [PubMed]
5. Lu, Y.; Zeng, Y.; Wang, W. Relation disentanglement, the potential risk assessment, and source identification of heavy metals in the sediment of the Changzhao Reservoir, Zhejiang Province. *Environ. Sci. Pollut. Res.* **2023**, *30*, 82625–82636. [CrossRef] [PubMed]
6. Rovira, A.; Ibàñez, C. Sediment management options for the lower Ebro River and its delta. *J. Soils Sediments* **2007**, *7*, 285–295. [CrossRef]
7. Kondolf, G.M.; Gao, Y.; Annandale, G.W.; Morris, G.L.; Jiang, E.; Zhang, J.; Cao, Y.; Carling, P.; Fu, K.; Guo, Q.; et al. Sustainable sediment management in reservoirs and regulated rivers: Experiences from five continents. *Earth's Future* **2014**, *2*, 256–280. [CrossRef]
8. Mirauda, D.; Pannone, M.; De Vincenzo, A. An entropic model for the assessment of streamwise velocity dip in wide open channels. *Entropy* **2018**, *20*, 69. [CrossRef]
9. Covelli, C.; Cimorelli, L.; Pagliuca, D.N.; Molino, B.; Pianese, D. Assessment of erosion in river basins: A distributed model to estimate the sediment production over watersheds by a 3-Dimensional LS Factor in RUSLE Model. *Hydrology* **2020**, *7*, 13. [CrossRef]
10. Cimorelli, L.; Covelli, C.; De Vincenzo, A.; Pianese, D.; Molino, B. Sedimentation in reservoirs: Evaluation of return periods related to operational failures of water supply reservoirs with Monte Carlo simulation. *J. Water Resour. Plan. Manag.* **2021**, *147*, 04020096. [CrossRef]
11. Anari, R.; Gaston, T.L.; Randle, T.J.; Hotchkiss, R.H. New Economic Paradigm for Sustainable Reservoir Sediment Management. *J. Water Resour. Plan. Manag.* **2023**, *149*, 04022078. [CrossRef]
12. de Araújo, J.C.; Landwehr, T.; Alencar, P.H.L.; Paulino, W.D. Water Management causes increment of reservoir silting and reduction of water yield in the semiarid State of Ceará, Brazil. *J. S. Am. Earth Sci.* **2023**, *121*, 104102. [CrossRef]
13. Carone, M.T.; Greco, M.; Molino, B. A sediment-filter ecosystem for reservoir rehabilitation. *Ecol. Eng.* **2006**, *26*, 182–189. [CrossRef]

14. Randle, T.J.; Morris, G.L.; Tullos, D.D.; Weirich, F.H.; Kondolf, G.M.; Moriasi, D.N.; Annandale, G.W.; Fripp, J.; Minear, J.T.; Wegner, D.L. Sustaining United States reservoir storage capacity: Need for a new paradigm. *J. Hydrol.* **2021**, *602*, 126686. [CrossRef]
15. Morris, G.L.; Fan, J. *Reservoir Sedimentation Handbook*; McGraw-Hill Book Co.: New York, NY, USA, 1998; ISBN 0-07-043302-X.
16. Asthana, B.N.; Khare, D. Reservoir sedimentation. In *Recent Advances in Dam Engineering*; Springer: Cham, Switzerland, 2022; pp. 265–288. [CrossRef]
17. De Vincenzo, A.; Molino, B. The rehabilitation of a reservoir: A new methodological approach for calculating the sustainable useful storage capacity. *Agric. Sci.* **2013**, *4*, 46–50. [CrossRef]
18. Djeran-Maigre, I.; Razakamanantsoa, A.; Levacher, D.; Hussain, M.; Delfosse, E. A relevant characterization of Usumacinta river sediments for a reuse in earthen construction and agriculture. *J. S. Am. Earth Sci.* **2023**, *125*, 104317. [CrossRef]
19. Bortali, M.; Rabouli, M.; Yessari, M.; Hajjaji, A. Characterizing harbor dredged sediment for sustainable reuse as construction material. *Sustainability* **2023**, *15*, 1834. [CrossRef]
20. Ben Allal, L.; Ammari, M.; Frar, I.; Azmani, A.; Belmokhtar, N.E. Caractérisation et valorisation des sédiments de dragage des ports de Tanger et Larache (Maroc). *Revue Paralia* **2011**, *4*, 5.1–5.13. [CrossRef]
21. Gouré-Doubi, H.; Lecomte-Nana, G.; Thery, F.; Peyratout, C.; Anger, B.; Levacher, D. Characterization and valorization of dam sediment as ceramic materials. *Int. J. Eng. Innov. Technol.* **2015**, *4*, 84–91.
22. Haurine, F.; Cojan, I.; Bruneaux, M.A. Development of an industrial mineralogical framework to evaluate mixtures from reservoir sediments for recovery by the heavy clay industry: Application of the Durance system (France). *Appl. Clay Sci.* **2016**, *132*, 508–517. [CrossRef]
23. Faure, A.; Coudray, C.; Anger, B.; Moulin, I.; Colina, H.; Izoret, L.; Théry, F.; Smith, A. Beneficial reuse of dam fine sediments as clinker raw material. *Constr. Build. Mater.* **2019**, *218*, 365–384. [CrossRef]
24. Mesrar, L.; Benamar, A.; Duchemin, B.; Brasselet, S.; Bourdin, F.; Jabrane, R. Engineering properties of dredged sediments as a raw resource for fired bricks. *Bull. Eng. Geol. Environ.* **2021**, *80*, 2643–2658. [CrossRef]
25. Martínez-Alvarez, V.; Gonz'alez-Ortega, M.J.; Martin-Gorriz, B.; Soto-García, M.; Maestre-Valero, J.F. Seawater desalination for crop irrigation-current status and perspectives. In *Emerging Technologies for Sustainable Desalination Handbook*, 1st ed.; Gude, G., Ed.; Butterworth-Heinemann: Oxford, UK, 2018; pp. 461–492. [CrossRef]
26. Nikafkar, N.; Alroaia, Y.V.; Heydariyeh, S.A.; Schleiss, A.J. Economic and commercial analysis of reusing dam reservoir sediments. *Ecol. Econ.* **2023**, *204*, 107668. [CrossRef]
27. Chahal, H.; Pothier, C.; Djeran-Maigre, I. Study of Landfills Using GCL for PCB Contaminated Sediments. In Proceedings of the 5th European Geosynthetics Congress, Valencia, Spain, 16–19 September 2012.
28. Chahal, H. Étude du comportement hydromécanique des sédiments pollués par les Poly-Chloro-Biphényles en interaction avec les géomatériaux pour un stockage hors site. Ph.D. Thesis, PhD-INSA Lyon, Lyon, France, 23 July 2013. (In French).
29. Kutlu, B. Contamination and ecological risk assessment of heavy metals in surface sediments of the Munzur stream, Turkey. *Pol. J. Environ. Stud.* **2023**, *32*, 587–597. [CrossRef] [PubMed]
30. Bagarani, M.; De Vincenzo, A.; Ievoli, C.; Molino, B. The reuse of sediments dredged from artificial reservoirs for beach nourishment: Technical and economic feasibility. *Sustainability* **2020**, *12*, 6820. [CrossRef]
31. Zhang, T.; Wang, M.; Bai, G.; Liu, J.; Li, P.; Zhang, Y.; Xia, S. Distribution characteristics, risk assessment, and source analysis of heavy metals in surface sediments and near-lakeshore soils of a plateau lake in China. *Gondwana Res.* **2023**, *115*, 191–200. [CrossRef]
32. Zonta, R.; Zaggia, L.; Argese, E. Heavy metal and grain-size distributions in estuarine shallow water sediments of the Cona Marsh (Venice Lagoon, Italy). *Sci. Total Environ.* **1994**, *151*, 19–28. [CrossRef]
33. Chen, C.W.; Kao, C.M.; Chen, C.F.; Dong, C.D. Distribution and accumulation of heavy metals in the sediments of Kaohsiung Harbor, Taiwan. *Chemosphere* **2007**, *66*, 1431–1440. [CrossRef]
34. Minello, M.C.S.; Paco, A.L.; Martines, M.A.U.; Caetano, L.; Santos, A.D.; Padilha, P.M.; Castro, G.R. Sediment grain size distribution and heavy metals determination in a dam on the Paraná River at Ilha Solteira, Brazil. *J. Environ. Sci. Health* **2009**, *44 Pt A*, 861–865. [CrossRef]
35. Lai, T.M.; Lee, W.; Hur, J.; Kim, Y.; Huh, I.A.; Shin, H.S.; Lee, J.H. Influence of sediment grain size and land use on the distributions of heavy metals in sediments of the Han River Basin in Korea and the assessment of anthropogenic pollution. *Water Air Soil Pollut.* **2013**, *224*, 1609. [CrossRef]
36. Abdallah, M.A.M. Accumulation and distribution of heavy metals in surface sediments from the continental shelf adjacent to Abu Qir Bay, Egypt, as a function of grain size. *Geo-Mar. Lett.* **2023**, *43*, 2. [CrossRef]
37. Xiao, T.; Ran, F.; Li, Z.; Wang, S.; Nie, X.; Liu, Y.; Feng, S. Sediment organic carbon dynamics response to land use change in diverse watershed anthropogenic activities. *Environ. Int.* **2023**, *172*, 107788. [CrossRef]
38. Asomba, H.C.; Ezewudo, B.I.; Okeke, C.J.; Islam, M.S. Grain size analysis and ecological risk assessment of metals in the sediments of Konsin River and Igboho dam reservoir, Oyo State, Nigeria, under agricultural disturbances. *Environ. Monit. Assess.* **2023**, *195*, 378. [CrossRef] [PubMed]
39. Verma, S.; Verma, M.K.; Prasad, A.D.; Mehta, D.; Azamathulla, H.M.; Muttil, N.; Rathnayake, U. Simulating the hydrological processes under multiple land use/land cover and climate change scenarios in the mahanadi reservoir complex, Chhattisgarh, India. *Water* **2023**, *15*, 3068. [CrossRef]

40. He, D.; Shi, X.; Wu, D. Particle-size distribution characteristics and pollution of heavy metals in the surface sediments of Kuitun River in Xinjiang, China. *Environ. Earth Sci.* **2016**, *75*, 272–282. [CrossRef]
41. Baran, A.; Tack, F.M.; Delemazure, A.; Wieczorek, J.; Tarnawski, M.; Birch, G. Metal contamination in sediments of dam reservoirs: A multi-facetted generic risk assessment. *Chemosphere* **2023**, *310*, 136760. [CrossRef] [PubMed]
42. Liu, Y.; Zhou, Z.; Gong, W.; Xu, Y.; Ding, Q.; Cui, L. Distribution, risk assessment of heavy metals in sediments, and their potential risk on water supply safety of a drinking water reservoir, middle China. *Environ. Sci. Pollut. Res.* **2023**, *30*, 73702–73713. [CrossRef] [PubMed]
43. Liang, R.Z.; Gu, Y.G.; Li, H.S.; Han, Y.J.; Niu, J.; Su, H.; Jiang, S.J. Multi-index assessment of heavy metal contamination in surface sediments of the Pearl River estuary intertidal zone. *Mar. Pollut. Bull.* **2023**, *186*, 114445. [CrossRef]
44. Wang, W.; Wu, F.; Yin, T.; Jiang, S.; Tang, S. Distribution, source, and contamination assessment of heavy metals in surface sediments of the Zhifu Bay in northern China. *Mar. Pollut. Bull.* **2023**, *194*, 115449. [CrossRef]
45. Islam, M.S.; Shammi, R.S.; Jannat, R.; Kabir, M.H.; Islam, M.S. Spatial distribution and ecological risk of heavy metal in surface sediment of Old Brahmaputra River, Bangladesh. *Chem. Ecol.* **2023**, *39*, 173–201. [CrossRef]
46. Italian Presidential Decree n. 120/2017. Available online: https://www.gazzettaufficiale.it/eli/id/2017/08/07/17G00135/sg (accessed on 5 December 2023).
47. Zhang, J.; Chen, S.; Deng, H.; Wu, A.; Sun, W.; Chen, Y. Heavy metal concentrations and pollution assessment of riparian soils in Shandong Province. *Acta Ecol. Sin.* **2012**, *32*, 3144–3153. [CrossRef]
48. Shi, X.; Wang, J. Comparison of different methods for assessing heavy metal contamination in street dust of Xianyang City, NW China. *Environ. Earth Sci.* **2013**, *68*, 2409–2415. [CrossRef]
49. Italian Decree n. 152/2006. Available online: https://www.gazzettaufficiale.it/dettaglio/codici/materiaAmbientale (accessed on 5 December 2023).
50. Shapiro, S.S.; Wilk, M.B. An analysis of variance test for normality (complete samples). *Biometrika* **1965**, *52*, 591–611. [CrossRef]
51. Royston, P. Approximating the Shapiro-Wilk W-test for non-normality. *Stat. Comput.* **1992**, *2*, 117–119. [CrossRef]
52. Hanusz, Z.; Tarasinska, J.; Zielinski, W. Shapiro-Wilk test with known mean. *Revstat Stat. J.* **2016**, *14*, 89–100. [CrossRef]
53. Upton, G.J. Fisher's exact test. *J. R. Stat. Soc. Ser. A Stat. Soc.* **1992**, *155*, 395–402. [CrossRef]
54. Efron, B. Student's *t*-test under symmetry conditions. *J. Am. Stat. Assoc.* **1969**, *64*, 1278–1302. [CrossRef]
55. De Winter, J.C. Using the Student's *t*-test with extremely small sample sizes. *Pract. Assess. Res. Eval.* **2019**, *18*, 10. [CrossRef]
56. Tikuye, B.G.; Gill, L.; Rusnak, M.; Manjunatha, B.R. Modelling the impacts of changing land use and climate on sediment and nutrient retention in Lake Tana Basin, Upper Blue Nile River Basin, Ethiopia. *Ecol. Modell.* **2023**, *482*, 110383. [CrossRef]
57. Kabata-Pendias, A. *Trace Elements in Soils and Plants*, 3rd ed.; CRC Press: Boca Raton, FL, USA, 2000. [CrossRef]
58. Alloway, B.J. *Heavy Metals in Soils: Trace Metals and Metalloids in Soils and Their Bioavailability*; Springer Science & Business Media: Dordrecht, The Netherlands, 2012; Volume 22. [CrossRef]
59. Horowitz, A.J.; Stephens, V.C. The effects of land use on fluvial sediment chemistry for the conterminous US-Results from the first cycle of the NAWQA Program: Trace and major elements, phosphorus, carbon, and sulfur. *Sci. Total Environ.* **2008**, *400*, 290–314. [CrossRef]
60. Wang, X.; Han, J.; Xu, L.; Gao, J.; Zhang, Q. Effects of anthropogenic activities on chemical contamination within the Grand Canal, China. *Environ. Monit. Assess.* **2011**, *177*, 127–139. [CrossRef]
61. Dong, Q.; Song, C.; Yang, D.; Zhao, Y.; Yan, M. Spatial distribution, contamination assessment and origin of soil heavy metals in the Danjiangkou reservoir, China. *Int. J. Environ. Res. Public Health* **2023**, *20*, 3443. [CrossRef] [PubMed]
62. Martellotta, A.M.N.; Petrella, A.; Gentile, F.; Levacher, D.; Piccinni, A.F. Reuse of lake sediments in sustainable mortar. *Environments* **2023**, *10*, 149. [CrossRef]
63. Junakova, N.; Junak, J. Recycling of reservoir sediment material as a binder in concrete. *Procedia Eng.* **2017**, *180*, 1292–1297. [CrossRef]